Linking nuclear formation processes and stellar chemical surface composition.

GSI

Camilla Juul Hansen

The Dark Cosmology Centre, University of Copenhagen

January 2016

Outline

- *Cool stars are the only astrophysical objects in which we can conduct a detailed and precise abundance study of up to ∼70 elements*
- Stellar parameters, abundances, and assumptions
- Tracing the astrophysical formation site using stellar abundances
- Meteorites
- CEMP stars
- Galactic chemical evolution
- Yield predictions

Very Large Telescope (VLT) - 8-m mirror

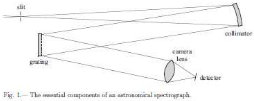

Figure: Simple sketch of a spectrograph – Massey et al.

Large Sky Area Multi-Object Fiber Spectroscopic Telescope (LAMOST) — 4-m mirror, 4000 fibres → 10000 stars/night or $2 \cdot 10^6$ stars/year → *Surveys*

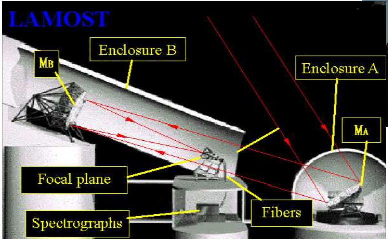

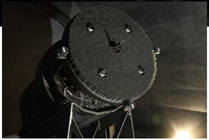

LAMOST vs UVES/VLT spectra

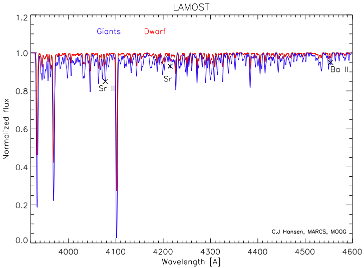

Figure: LAMOST (low resolution $R \sim 1800$) and ESO VLT (UVES - high resolution $R \sim 40000$)

LAMOST vs UVES/VLT spectra

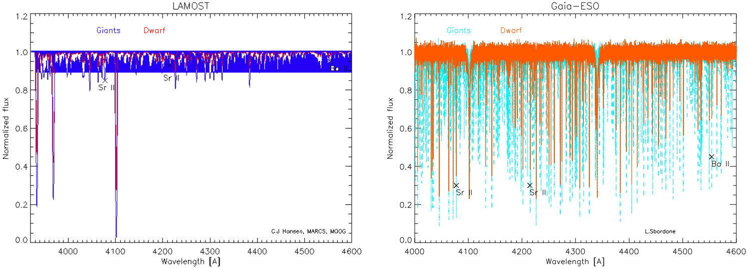

Figure: LAMOST (low resolution $R \sim 1800$) with noise and ESO VLT (UVES - high resolution $R \sim 40000$)

Important: Sr may be the only heavy element for which we will be able to derive abundances in low-resolution spectra.

Stellar spectra – 2D to 1D

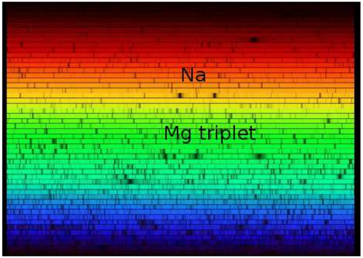

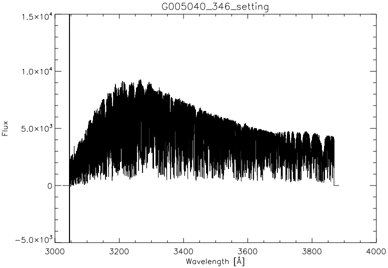

Stellar spectra and equivalent width (W)

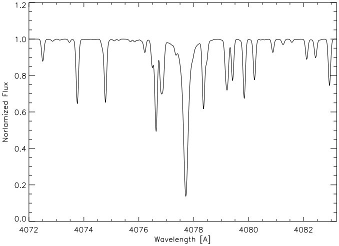

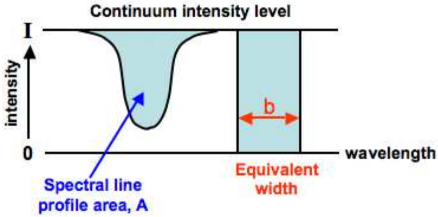

Abundance - W - log gf relation; the impact of stellar parameters and atomic data

$$\log \mathrm{W} = \log(const) + \log(A) + \log(gf\lambda) - \theta\chi - \log(\kappa) \qquad (1)$$

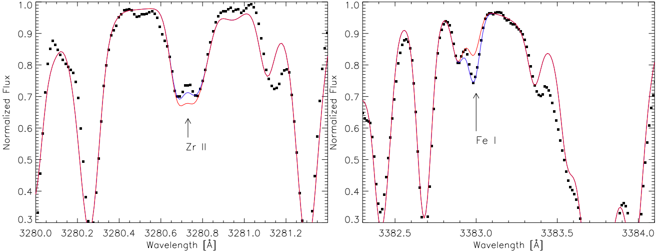

Hansen et al, 2012

Since the UV-region of the spectra is crowded we have to carry out spectral synthesis on line lists with accurate atomic data.

Two ways of deriving abundances:

- Equivalent width and synthetic spectra
- We need to know the stellar parameters: Temperature, gravity, metallicity and velocity (small scale)
- Model atmosphere (e.g. MARCS) and synthetic spectrum code (e.g. MOOG)
- Assumptions: 1D, LTE – one local temperature, black body radiation (Planck), Maxwellian velocity distribution, Boltzmann and Saha describe excitation and ionisation
- Line lists with atomic and molecular information (excitation potential and log gf)

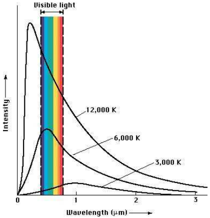

Temperature, gravity and metallicity

- The color of a star depends on two factors: Temperature and metallicity
- Color (V-K) calibration Alonso et al. 1999, Casagrande et al. 2010:
  $T = a + b(V-K) + c(V-K)^2 + d(V-K)[Fe/H] + ...$
- Excitation potential - based on Fe lines (NLTE sensitive)
- Parallax/distance (π) e.g., Nissen et al. 1997:
  $log\frac{g}{g_{Sun}} = log\frac{M}{M_{Sun}} + 4\frac{T}{T_{Sun}} + 0.4V_o + 2log(\pi) + corrections$
- Ionisation equilibrium from Fe lines (NLTE sensitive)
- Metallicity ([Fe/H]) from equivalent widths of Fe lines

Abundances for Astronomers (spectroscopists)

$$\log \epsilon(Element) = \log(N_{Element}/N_H) + 12 \tag{2}$$

where

$$\log(N_H) = 12 \tag{3}$$

Abundances for Theoreticians

X = H (mass fraction: ~ 0.75),
Y = He (~ 0.25), and
Z = Li and heavier (< 0.01)

Stellar spectra, abundances, and [Fe/H]

$$[\mathrm{Fe/H}] \equiv \log(N_{\mathrm{Fe}}/N_{\mathrm{H}})_* - \log(N_{\mathrm{Fe}}/N_{\mathrm{H}})_\odot \tag{4}$$

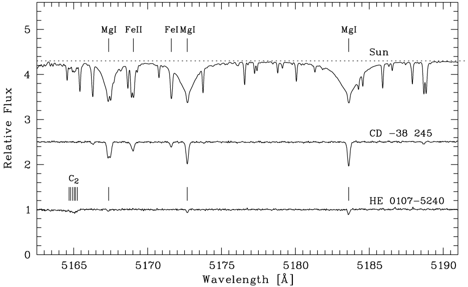

Figure: Top: Solar ([Fe/H] = 0) spectrum – Mg triplet. Bottom: Star with [Fe/H] $\sim$ -5. Christlieb +2004

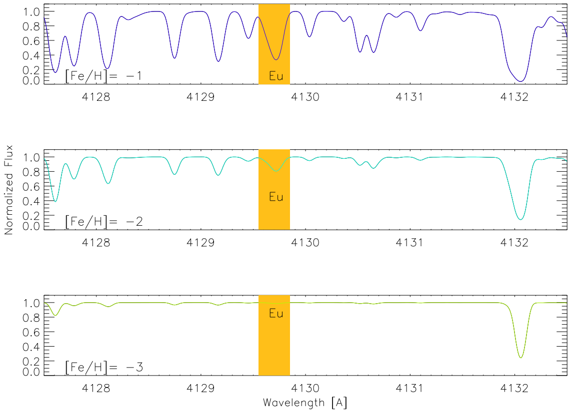

Figure: Observational abundance biases (Hansen et al, 2014b)

Observable elements - with high-resolution instruments

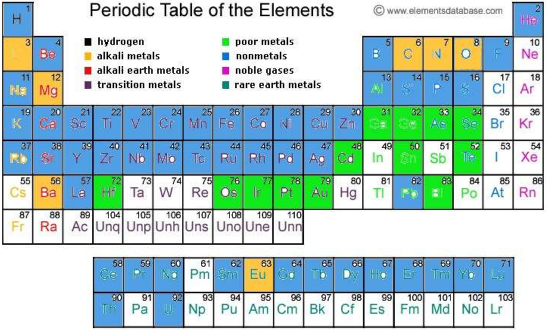

Figure: Blue: ground based observations, green: space, yellow: isotopic abundances

Record holding star
- CS31082-001
Abundances
of almost 70 elements,
37 of which are heavy elements.
Siqueira Mello et al. 2013

Table 1. LTE abundances in CS 31082-001 as derived from previous works, from the present paper, and our adopted final abundances.

El.	Z	A(X) (1)	A(X) (2)	A(X) (3)	A(X) This Work	A(X) adopted	[X/Fe] adopted
Ge	32	—	—	—	+0.10	+0.10±0.21	-0.55
Sr	38	+0.72	—	—	—	+0.72±0.10	0.73
Y	39	-0.23	—	—	-0.15	-0.19±0.07	0.53
Zr	40	+0.43	—	—	+0.55	+0.49±0.08	0.84
Nb	41	-0.55	—	—	-0.52	-0.54±0.12	0.97
Mo	42	—	—	—	-0.11	-0.11±0.13	0.90
Ru	44	+0.36	—	—	+0.36	+0.36±0.12	1.45
Rh	45	-0.42	—	—	-0.42	-0.42±0.12	1.39
Pd	46	-0.05	—	—	-0.09	-0.09±0.07	1.18
Ag	47	-0.81	—	—	-0.84	-0.84±0.21	1.15
Ba	56	+0.40	—	—	—	+0.40±0.14	1.16
La	57	-0.60	-0.62	—	—	-0.62±0.05	1.17
Ce	58	-0.31	-0.29	—	-0.31	-0.29±0.05	1.03
Pr	59	-0.86	-0.79	—	—	-0.79±0.05	1.38
Nd	60	-0.13	-0.15	—	-0.21	-0.15±0.05	1.33
Sm	62	-0.51	-0.42	—	-0.42	-0.42±0.05	1.51
Eu	63	-0.76	-0.72	—	-0.75	-0.72±0.05	1.69
Gd	64	-0.27	-0.21	—	-0.29	-0.21±0.05	1.61
Tb	65	-1.26	-1.01	—	-1.00	-1.01±0.05	1.64
Dy	66	-0.21	-0.07	—	-0.12	-0.07±0.05	1.73
Ho	67	—	-0.80	—	—	-0.80±0.06	1.62
Er	68	-0.27	-0.30	—	-0.31	-0.30±0.05	1.67
Tm	69	-1.24	-1.15	—	-1.18	-1.15±0.05	1.64
Yb	70	—	-0.41	—	—	-0.41±0.11	1.66
Lu	71	—	—	—	-1.08	-1.08±0.13	1.73
Hf	72	-0.59	-0.72	—	-0.73	-0.72±0.05	1.33
Ta	73	—	—	—	-1.60	-1.60±0.23	1.47
W	74	—	—	—	-0.90	-0.90±0.24	0.92
Re	75	—	—	—	-0.21	-0.21±0.21	2.45
Os	76	+0.43	—	+0.18	—	+0.18±0.07	1.72
Ir	77	+0.20	—	+0.20	—	+0.20±0.07	1.72
Pt	78	—	—	+0.30	—	+0.30±0.23	1.46
Au	79	—	—	-1.00	—	-1.00±0.34	0.89
Pb	82	—	—	-0.65	—	-0.65±0.19	0.25
Bi	83	—	—	-0.40	—	-0.40±0.33	1.83
Th	90	-0.98	—	—	—	-0.98±0.13	1.84
U	92	-1.92	—	—	—	-1.92±0.17	1.68

References. (1) Hill et al. (2002), (2) Sneden et al. (2009), (3) Barbuy et al. (2011).

Another record holding star:

Keller et al. 2014: [Fe/H] < 7.1 - origin SN II of M$\sim 60 M_{\odot}$

Bessel et al. 2015 (3D, NLTE corrections) $\rightarrow 40 M_{\odot}$ SN

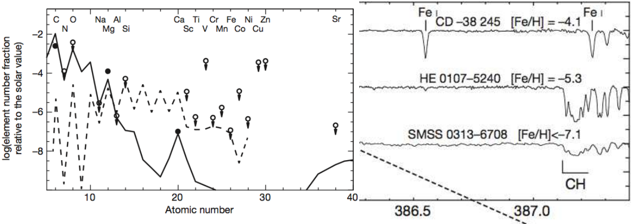

Figure 3 | The element abundance pattern for SMSS 0313−6708 compared

Sr GCE

- Big Bang Nucleosynthesis: H,He, and Li
- SN type II: α-elements
- SN type Ia: Fe-peak elements
- Neutron-capture processes (most heavy isotopes) SN, NSM, AGB,...

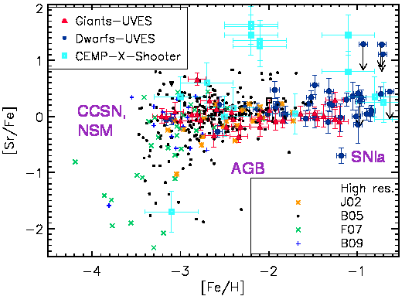

Assumptions: LTE vs NLTE - the impact on stellar parameters

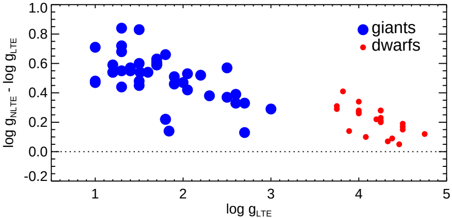

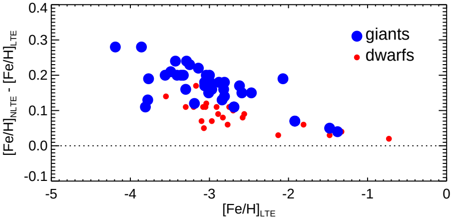

Figure: Hansen et al. 2013

Assumptions: LTE vs NLTE - Strontium

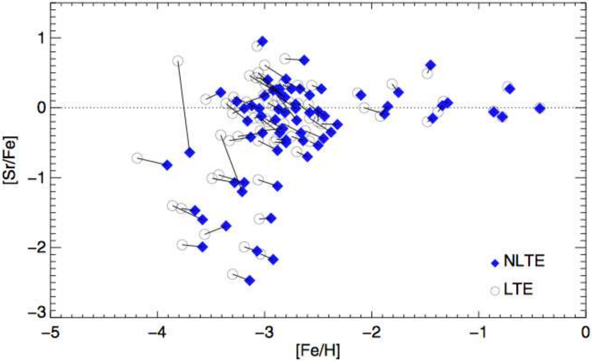

Figure: Hansen et al. 2013

Chemical evolution of Sr
Yields from faint SN II (Wanajo et al.) Hansen et al. 2013

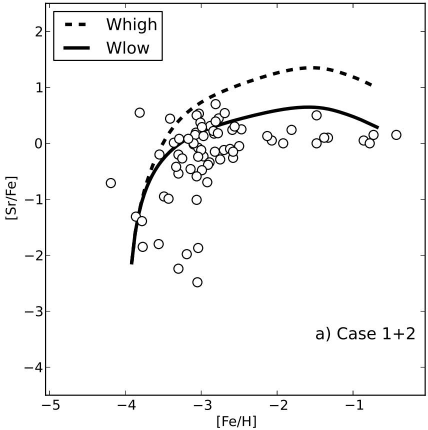

Chemical evolution of Sr
Yields from ν–driven winds (Arcones & Montes) Hansen et al. 2013

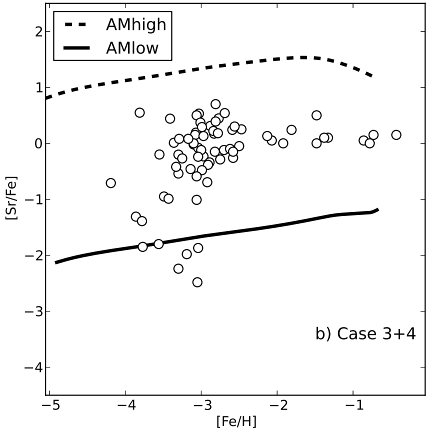

Chemical evolution of Sr
Yields from massive fast rotating stars (Frischknecht et al.) Hansen et al. 2013

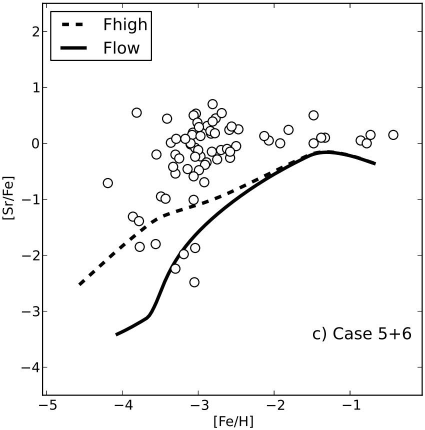

The chemical evolution of Sr – LTE vs NLTE

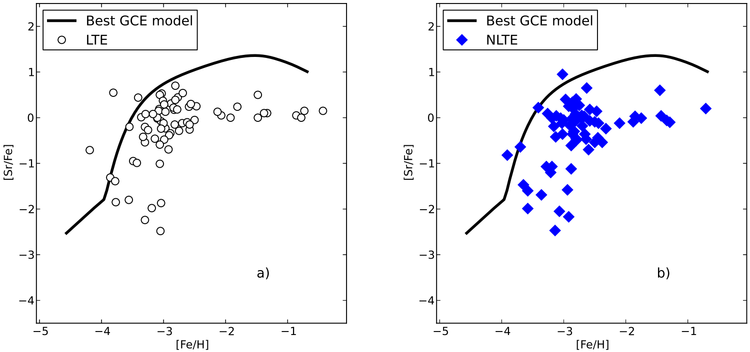

Figure: Hansen et al. 2013

The uncertain yields can cover a large range of stellar abundances. Despite uncertainties we can still make quantitative predictions such as:

- Massive stars may facilitate an early s-process which creates small amounts of Sr.
- Faint CC SN are well constrained due to the selfconsistent 2D models and match the observations fairly well (despite slight overpredictions).
- ν-driven winds are promising but need to be better constrained.

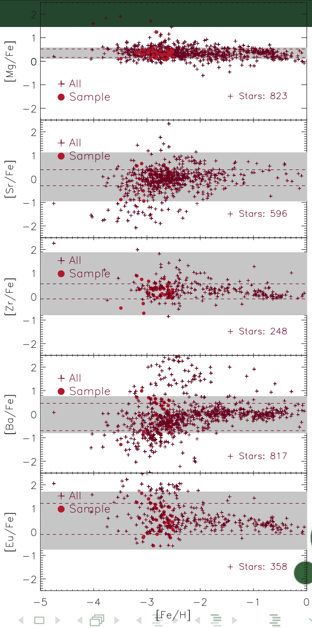

Scatter and multiple formation processes

- Weak s-process: $Z \sim< 40$ (or 42)
- Main s-process - broad atomic range - typically Ba ($Z = 56$) and heavier
- Weak r-process: $40 < Z < 50$
- Main r-process - possibly full range - or $Z > 50$ (Hansen et al. 2014b)

Abundance star-to-star scatter and the 2nd/weak r-process

- HD122563 - proto weak r star
- Large star-to-star scatter for n-capture elements (e.g. Sr & Ba)

Figure: Hansen et al. 2011, 2012, Cowan et al. 2011 (below)

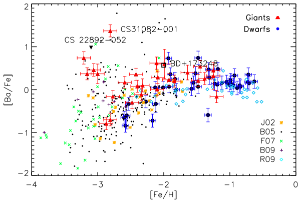

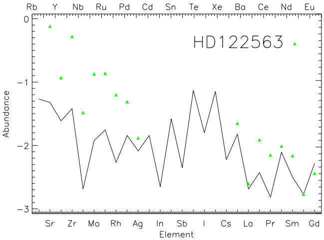

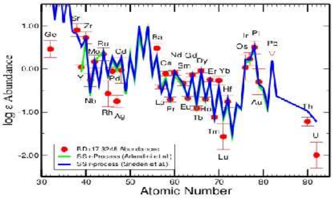

Selected elements

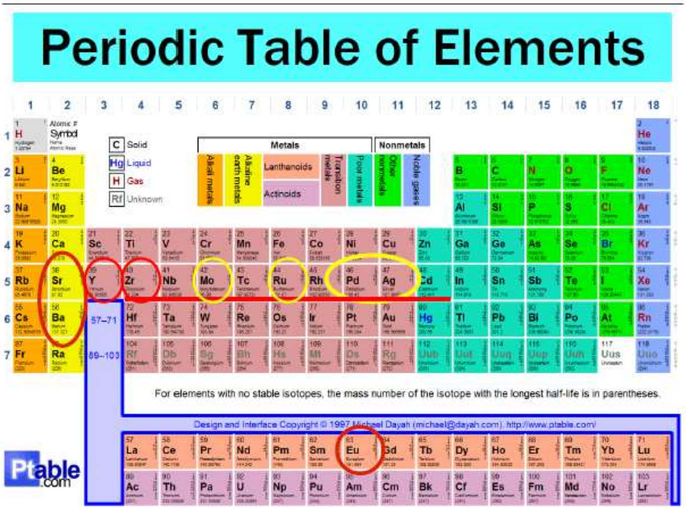

Near-UV – blue spectra (Hansen et al. 2012, 2014a)

$$\log \mathrm{W} = \log(const) + \log(A) + \log(gf\lambda) - \theta\chi - \log(\kappa) \quad (5)$$

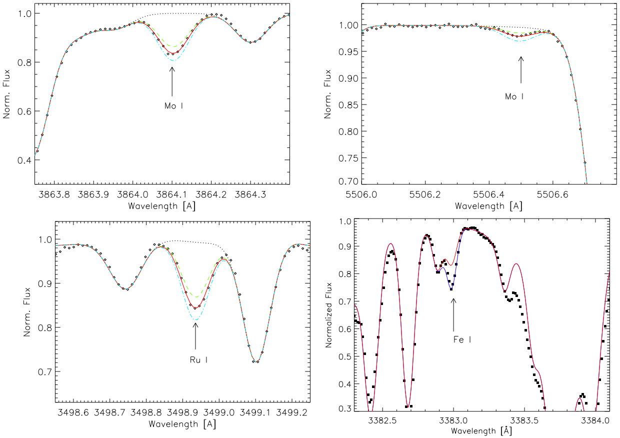

Galactic chemical evolution of Mo and Ru

$$[\mathrm{Fe/H}] \equiv \log(N_{\mathrm{Fe}}/N_{\mathrm{H}})_* - \log(N_{\mathrm{Fe}}/N_{\mathrm{H}})_\odot \qquad (6)$$

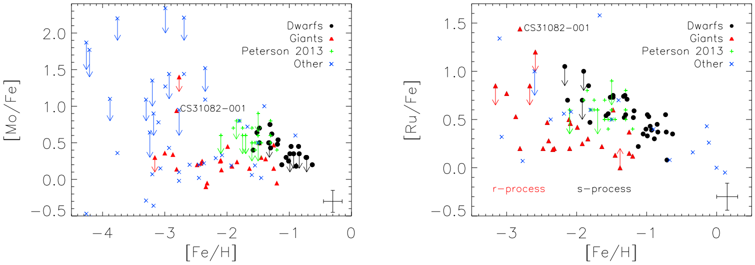

Figure: Hansen et al, 2014

Galactic chemical evolution of Pd and Ag

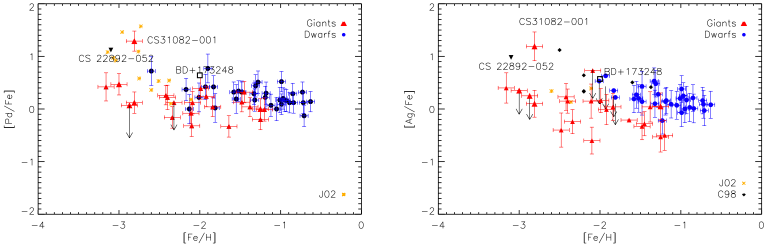

Figure: **Hansen et al, 2012**

r-poor vs r-rich stars: HD122563 & CS31082-001

(Honda et al,2006, Hill et al, 2002 & Hansen et al, 2012)

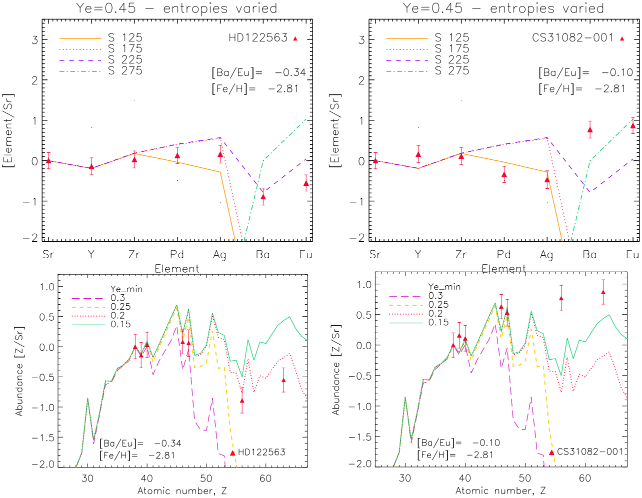

Correlation - Anticorrelation

If two elements are created by the same process, they most likely grow in the same way (correlate).

Elements ($38 < Z < 50$) are generally found to anti-correlate with $Z > 56$ elements (Burris et al, 2000, Montes et al, 2007, Francois et al 2007)

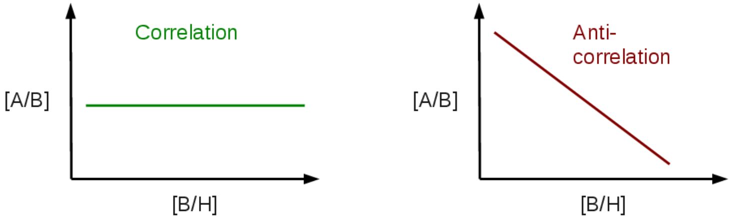

Weak/main s/r-process elements - Sr (85% s), Ba (81% s) and Eu (94% r) Arlandini et al 1999 Hansen et al, 2012

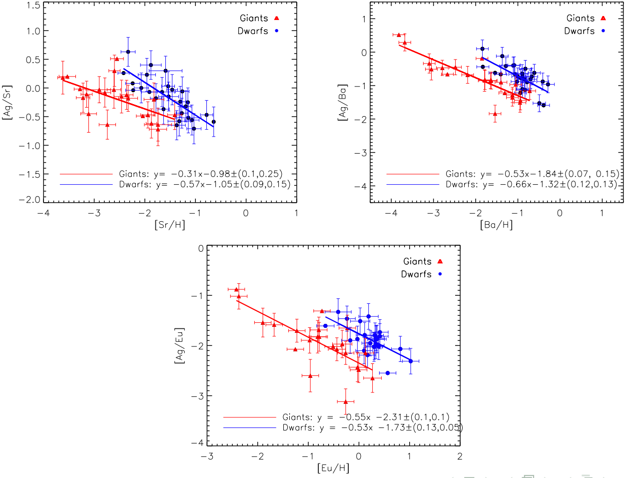

Weak r-process elements: Ru, Pd, and Ag Hansen et al 2012, 2014a

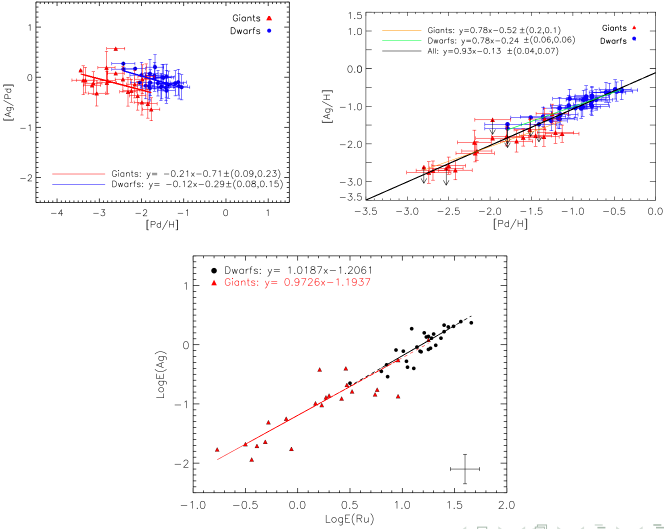

Ru not main s or main r (Hansen et al. 2014a)

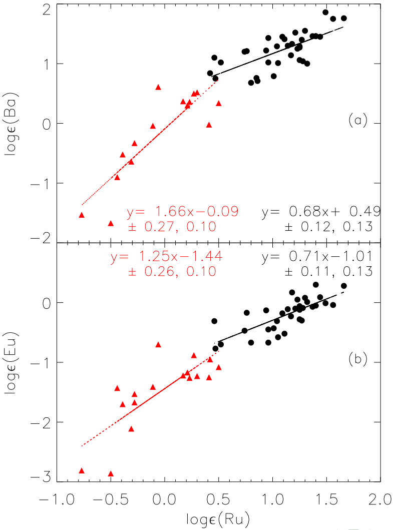

Two r-processes

Ru, Pd, and Ag are formed by the weak r-process

- The main r-process creates the heaviest elements (Z > 56) in a very robust way
- The 'weak' r-process creates the intermediately heavy ($37 <$ Z < 50) - range uncertain
- Possible formation sites are neutron star (NS) mergers (main r), and ECSN, ν-driven winds (weak r)

Comparing stars and meteorites
(Hansen et al. 2014a)

Element				Isotope			
Mo	92	94	95	96	97	98	100
Ru	96	98	99	100	101	102	104
Process	p	p	r + s	s	r + s	r + s	r

$$\log \epsilon = \log \left(\frac{\frac{^iX}{^jX}_{grain}}{\frac{^iX}{^jX}_{A\&G}} \right) + 1.554.$$

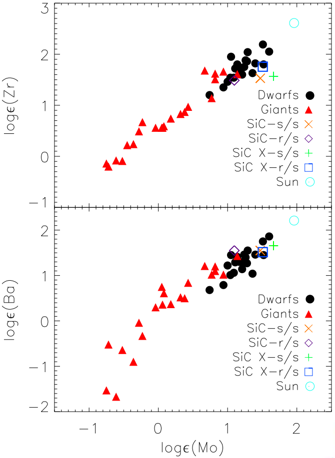

CEMP - why care?

Between 40% and 100% of EMP stars are CEMP stars!

The ~ 10 most metal-poor stars known

Keller et al. 2014, Hansen (CJH) et al. 2015

and C-normal: Caffau et al. 2011

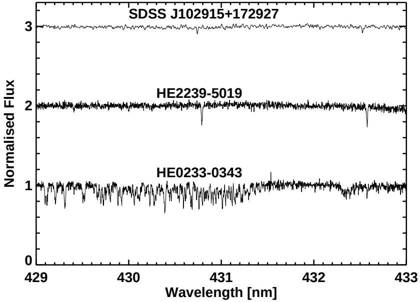

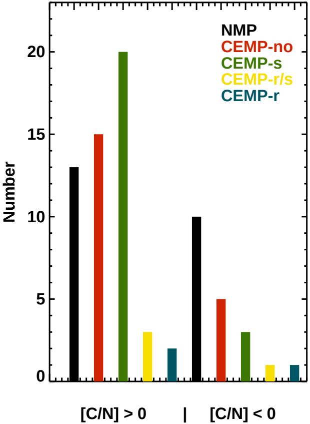

CEMP stars

TABLE 2 Definition of subclasses of metal-poor stars

Neutron-capture-rich stars	
r-I	0.3 ≤ [Eu/Fe] ≤ +1.0 and [Ba/Eu] < 0
r-II	[Eu/Fe] > +1.0 and [Ba/Eu] < 0
s	[Ba/Fe] > +1.0 and [Ba/Eu] > +0.5
r/s	0.0 < [Ba/Eu] < +0.5
Carbon-enhanced metal-poor stars	
CEMP	[C/Fe] > +1.0
CEMP-r	[C/Fe] > +1.0 and [Eu/Fe] > +1.0
CEMP-s	[C/Fe] > +1.0, [Ba/Fe] > +1.0, and [Ba/Eu] > +0.5
CEMP-r/s	[C/Fe] > +1.0 and 0.0 < [Ba/Eu] < +0.5
CEMP-no	[C/Fe] > +1.0 and [Ba/Fe] < 0

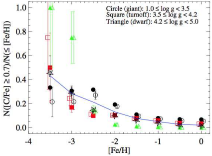

Figure 10. Cumulative frequencies of CEMP stars ([C/Fe] ⩾ +0.7) from the SDSS/SEGUE+LS sample, as a function of [Fe/H], for three different luminosity classes: giants (circles), main-sequence turnoff stars (squares), and dwarfs (triangles). We assume classifications based on the measured surface gravity—giant: 1.0 ⩽ log *g* < 3.5, turnoff: 3.5 ⩽ log *g* < 4.2, and dwarf: 4.2 ⩽

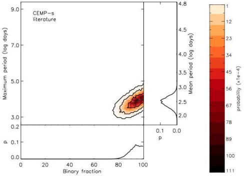

See, e.g., Beers & Christlieb 2005, Aoki et al. 2007, Masseron et al. 2010, Lugaro et al. 2012, Bisterzo 2010,2011, 2012

- Binary fraction increasing with decreasing metallicity.
- CEMP-no, CEMP-r $\sim 18\%$ & CEMP$-s$ - almost all $(> 80\%)$

  Lucatello et al. 2005, Lee et al. 2013, Starkenburg et al. 2014, Abate et a. 2015a,b, Hansen (T.T) et al. 2015b,c

CEMP-no and CEMP-s stars - unmixed dwarfs
(Spite et al. 2013)

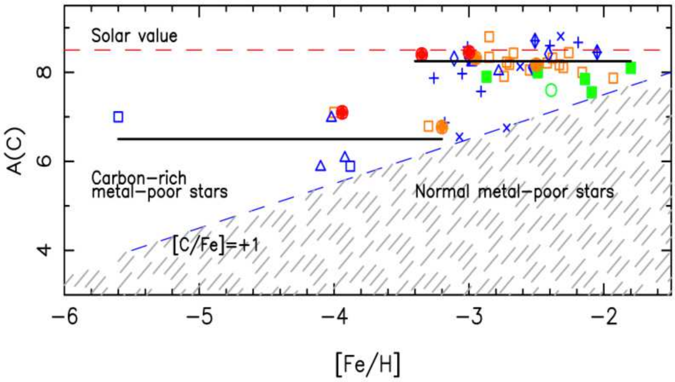

Fig. 14. Abundance of carbon A(C) vs. [Fe/H] in dwarfs and turnoff CEMP stars, following Sivarani et al. (2006, their Table 4), [orange open squares]), Frebel et al. (2005, 2007) [blue open squares], Thompson et al. (2008) [green open circle], Aoki et al. (2009) [blue open diamonds], Behara et al. (2010) [full orange circles], Placco et al.

CEMP-no and CEMP-s stars - Extremely/Ultra metal-poor stars

(Bonifacio et al. 2015)

Bonifacio et al.: TOPoS: II. C-enhanced stars

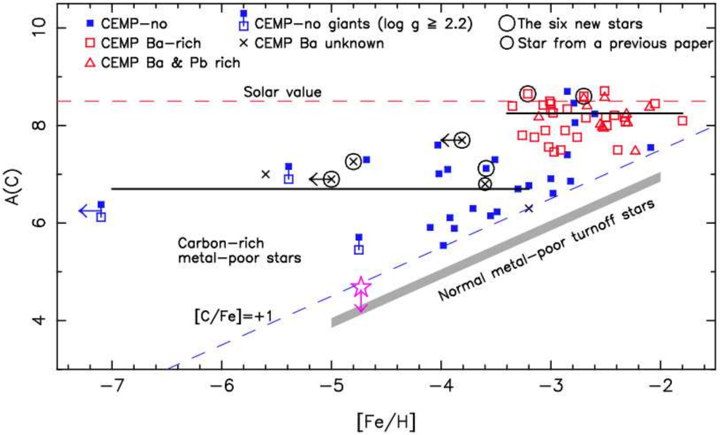

Fig. 6. The carbon abundances A(C) of CEMP stars as a function of [Fe/H]. The stars in the present paper and in Caffau et al. (2013a) are shown with big and small circles, respectively. The other turn-off stars come from the literature (Sivarani et al. 2006; Frebel et al. 2005, 2006; Thompson et al. 2008; Aoki et al. 2008; Behara et al. 2010; Masseron et al. 2010, 2012; Yong et al. 2013; Cohen et al. 2013; Li et al. 2015). The CEMP-no

X-shooter CEMP stars

(Hansen et al. 2016)

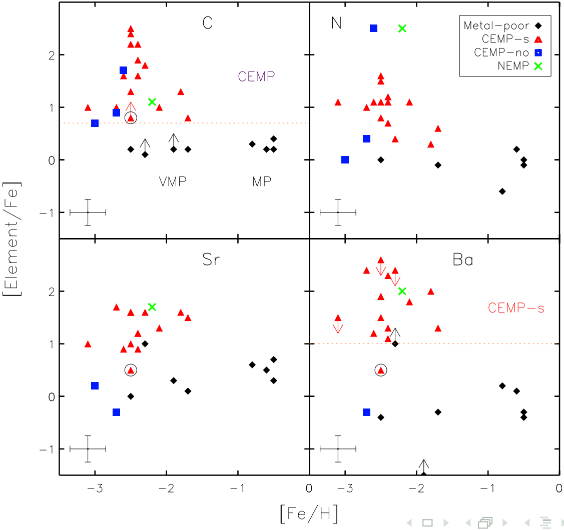

CEMP-s and -no stars - different from EMP C-normal stars

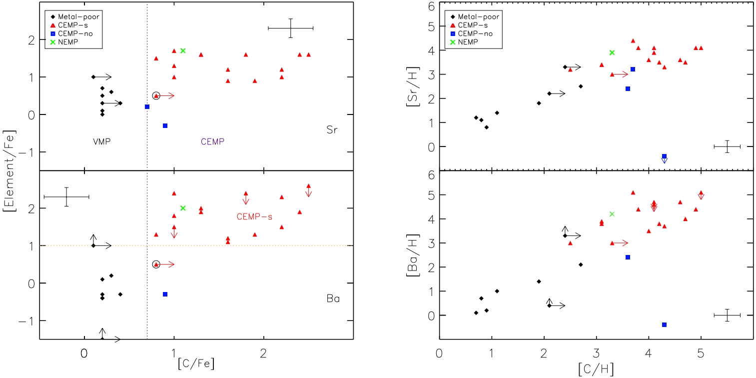

Figure: Hansen et al. 2016

CEMP-s and -no stars - different from EMP C-normal stars
This is in agreement with the recent findings Bonifacio et al. 2015

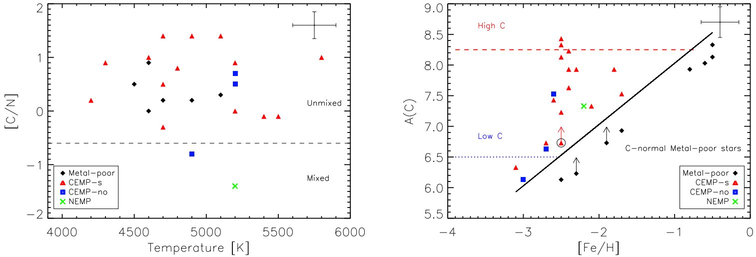

Figure: Hansen et al. 2016

CEMP-s vs -no stars - and C-normal stars

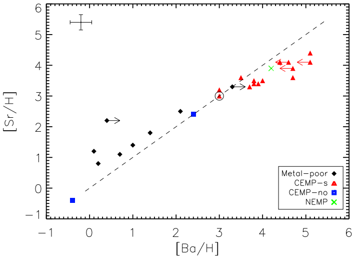

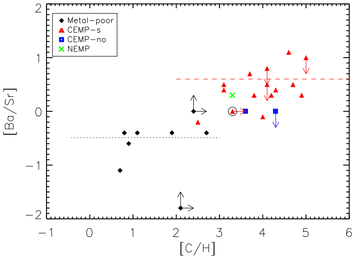

Figure: <[Ba/Sr]> ~ 0.5 for $\sim 2M_{\odot}$ AGB stars while <[Ba/Sr]> ~ -0.5 matches GCE prediction from spinstars (0 to -1.5). Hansen et al. 2016

GCE of CEMP and C-normal stars Predictions: Cescutti 2008, 2013

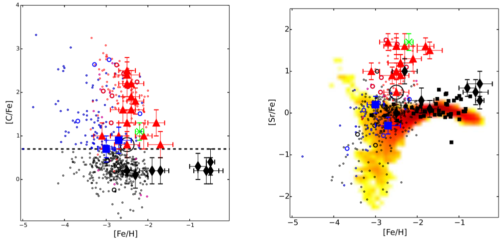

Figure: An r-process + spinstars ([Ba/Sr]~ 0 to -1.5). Hansen et al. 2016

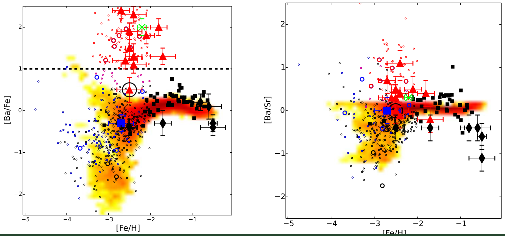

CEMP-r stars - fallback SN + AGB + ???

Hansen (CJH) et al. 2015

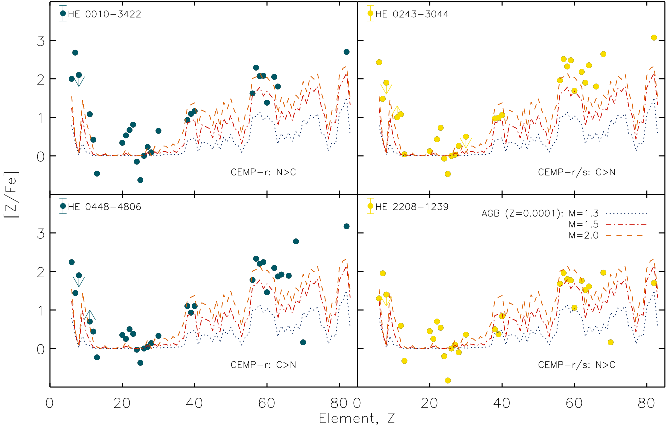

CEMP-s/r stars - i-process enriched?

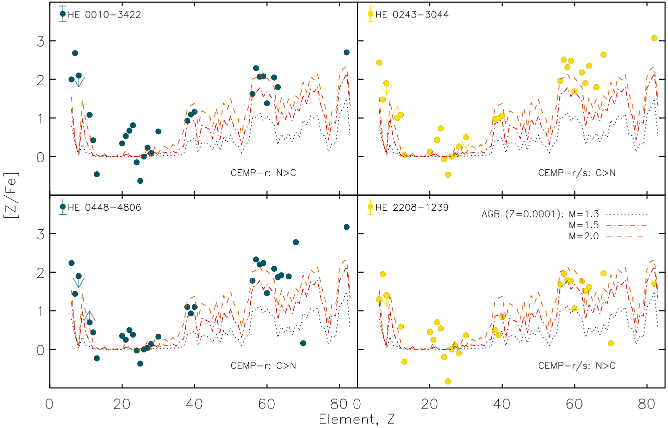

CEMP$-s/-r$ & intermediate $i-$process

- Massive (M$> 4M_\odot$) AGB stars (N enhancement via HBB Lau, Stancliffe & Tout, 2009)
- Models of massive AGB stars predict too low C/N-ratios and too low hs/ls-ratios compared to observations.
- FRUITY AGB yields Cristallo et al. 2011, 2015 match CEMP$-s$ stars, but not CEMP$-s/r$
- The CEMP$-s/r$ stars can be reproduced by an ($i-$)process e.g., Abate+ 2015a,b, Mishenina+ 2015,

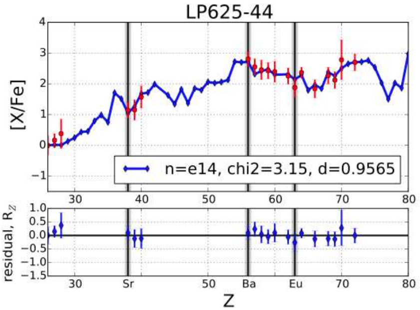

Figure: Hampel et al. 2016 in prep.

Assumptions (C-normal stars):
There are 2 robust processes:
main r-process (H), weak r (L).
M1: H=CS22892-052, L=HD122563
M2:
H=CS22892-052, H+L = HD122563
M3:
H+L=CS22892-052, H+L=HD122563
- all stars are mixed Li et al. 2013

$$Y_{calc}(Z) = (C_H Y_H(Z) + C_L Y_L(Z)) * 10^{[Fe/H]}$$

(Hansen et al. 2014b)

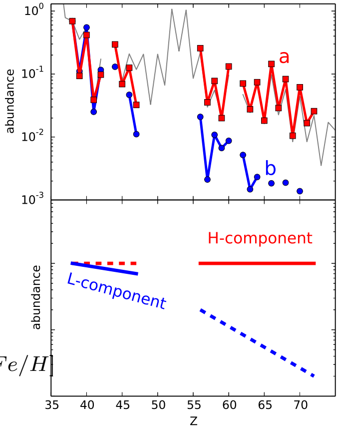

Assumptions:
There are 2 robust processes:
main r-process (H), weak r (L).
M1: H=CS22892-052, L=HD122563
M2: H=CS22892-052, H+L = HD122563
M3: H+L=CS22892-052, H+L=HD122563
- all stars are mixed

$$Y_{calc}(Z) = (C_H Y_H(Z) + C_L Y_L(Z)) * 10^{[Fe/H]}$$

(Hansen et al. 2014b)

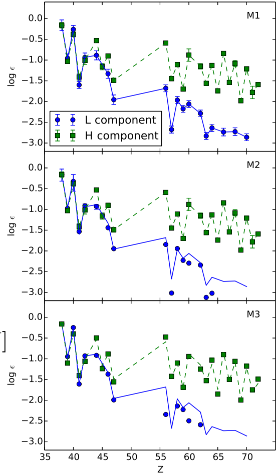

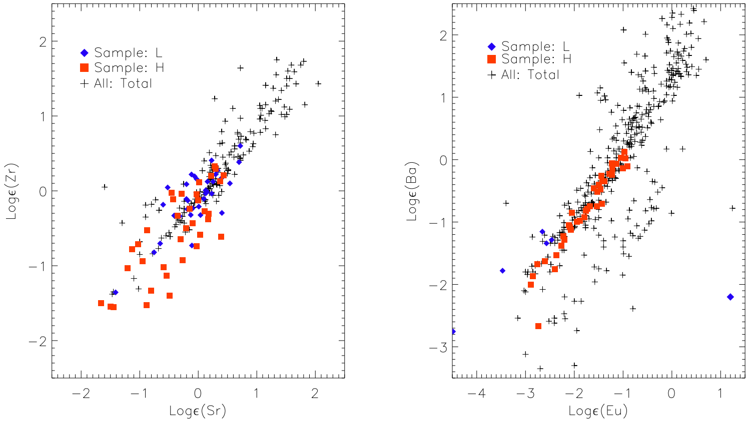

Figure: Robustness of the processes! **(Hansen et al, 2014b)**

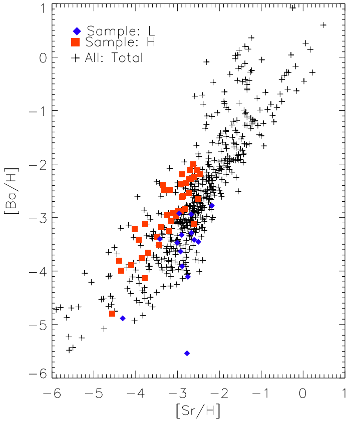

Figure: Differences in Sr and Ba (Hansen et al, 2014b)

Winds

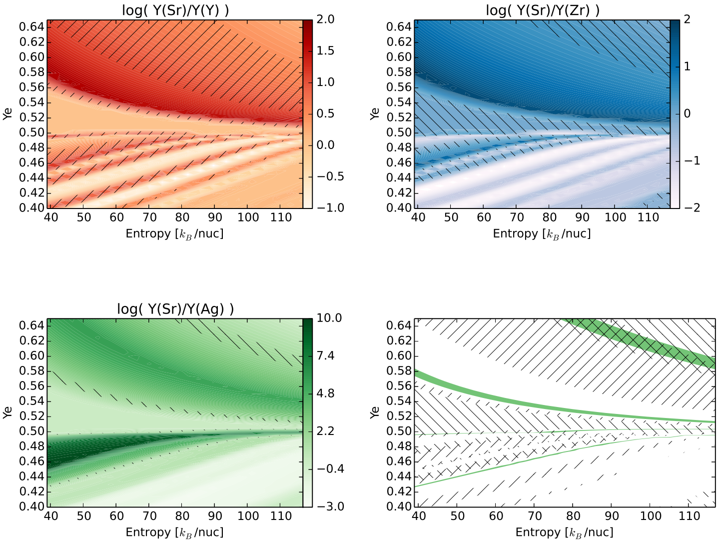
log(Y(Sr)/Y(Y))
log(Y(Sr)/Y(Zr))
log(Y(Sr)/Y(Ag))
Ye
Entropy [k_B/nuc]
0.64
0.62
0.60
0.58
0.56
0.54
0.52
0.50
0.48
0.46
0.44
0.42
0.40
40 50 60 70 80 90 100 110
2.0 1.5 1.0 0.5 0.0 −0.5 −1.0
2 1 0 −1 −2
10.0 7.4 4.8 2.2 −0.4 −3.0

Conclusion:

- We can use stellar abundances to constrain the nuclear synthetic formation processes, but it is important to know how the 1D, LTE assumptions affect these abundances.
- The stellar abundances are accurate enough to allow for a distinction between the r- and s-processes confirmed by the meteoritic isotopic abundances.
- Some yield predictions are still very uncertain.
- The formation of some CEMP stars remains a puzzle.
- Outlook: 3D, NLTE corrected heavy element abundances. Better constrained yields based on self-consistent exploding SN models (3D). Large homogeneously analysed samples and more complete abundance patterns - not just for GCE of single elements - but the surveys can be used to find important targets for detailed blue follow-up observations.

Conclusion:

- We can use stellar abundances to constrain the nuclear synthetic formation processes, but it is important to know how the 1D, LTE assumptions affect these abundances.
- The stellar abundances are accurate enough to allow for a distinction between the r- and s-processes confirmed by the meteoritic isotopic abundances.
- Some yield predictions are still very uncertain.
- The formation of some CEMP stars remains a puzzle.
- Outlook: 3D, NLTE corrected heavy element abundances. Better constrained yields based on self-consistent exploding SN models (3D). Large homogeneously analysed samples and more complete abundance patterns - not just for GCE of single elements - but the surveys can be used to find important targets for detailed blue follow-up observations.

Conclusion:

- We can use stellar abundances to constrain the nuclear synthetic formation processes, but it is important to know how the 1D, LTE assumptions affect these abundances.
- The stellar abundances are accurate enough to allow for a distinction between the r- and s-processes confirmed by the meteoritic isotopic abundances.
- Some yield predictions are still very uncertain.
- The formation of some CEMP stars remains a puzzle.
- Outlook: 3D, NLTE corrected heavy element abundances. Better constrained yields based on self-consistent exploding SN models (3D). Large homogeneously analysed samples and more complete abundance patterns - not just for GCE of single elements - but the surveys can be used to find important targets for detailed blue follow-up observations.

Conclusion:

- We can use stellar abundances to constrain the nuclear synthetic formation processes, but it is important to know how the 1D, LTE assumptions affect these abundances.
- The stellar abundances are accurate enough to allow for a distinction between the r- and s-processes confirmed by the meteoritic isotopic abundances.
- Some yield predictions are still very uncertain.
- The formation of some CEMP stars remains a puzzle.
- Outlook: 3D, NLTE corrected heavy element abundances. Better constrained yields based on self-consistent exploding SN models (3D). Large homogeneously analysed samples and more complete abundance patterns - not just for GCE of single elements - but the surveys can be used to find important targets for detailed blue follow-up observations.

Conclusion:

- We can use stellar abundances to constrain the nuclear synthetic formation processes, but it is important to know how the 1D, LTE assumptions affect these abundances.
- The stellar abundances are accurate enough to allow for a distinction between the r- and s-processes confirmed by the meteoritic isotopic abundances.
- Some yield predictions are still very uncertain.
- The formation of some CEMP stars remains a puzzle.
- Outlook: 3D, NLTE corrected heavy element abundances. Better constrained yields based on self-consistent exploding SN models (3D). Large homogeneously analysed samples and more complete abundance patterns - not just for GCE of single elements - but the surveys can be used to find important targets for detailed blue follow-up observations.

Thank you for listening